Scientific Research Publishing

Advances in Nanoparticles, 2022, 11, 31-54
https://www.scirp.org/journal/anp
ISSN Online: 2169-0529
ISSN Print: 2169-0510

Bio-Fabrication of Silver Nanoparticles Using *Catha edulis* Extract: Procedure Optimization and Antimicrobial Efficacy Encountering Antibiotic-Resistant Pathogens

Abdulqawi A. Numan[1,2*], Mashhour Ahmed[3,4], Mansour S. A. Galil[1,2], Mohyeddine Al-Qubati[5,6], Ayman A. Raweh[7,8], Enas A. Helmi[7]

[1]Department of Chemistry, Faculty of Applied Sciences, Taiz University, Taiz, Yemen
[2]Department of Pharmacy, Faculty of Medical Sciences, Al-Janad University for Science and Technology, Taiz, Yemen.
[3]Department of Pharmaceutical Chemistry and Natural Products, University of Science and Technology (UST), Sana'a, Yemen
[4]Central for Research and Pharmaceutical Studies (CRPS), University of Science and Technology (UST), Sana'a, Yemen
[5]Department of Mechatronics, Faculty of Engineering and Information Technology, Al-Janad University for Science and Technology, Taiz, Yemen
[6]Department of Physics, Faculty of Applied Sciences, Taiz University, Taiz, Yemen
[7]Department of Microbiology, Faculty of Applied Sciences, Taiz University, Taiz, Yemen
[8]Department of Clinical Laboratory, Faculty of Medical Sciences, Al-Janad University for Science and Technology, Taiz, Yemen
Email: *abdulqawin7@gmail.com

How to cite this paper: Numan, A.A., Ahmed, M., Galil, M.S.A., Al-Qubati, M., Raweh, A.A. and Helmi, E.A. (2022) Bio-Fabrication of Silver Nanoparticles Using *Catha edulis* Extract: Procedure Optimization and Antimicrobial Efficacy Encountering Antibiotic-Resistant Pathogens. *Advances in Nanoparticles*, **11**, 31-54.
https://doi.org/10.4236/anp.2022.112004

Received: March 23, 2022
Accepted: May 28, 2022
Published: May 31, 2022

Abstract

The current study aimed to optimize a green synthesis procedure for fabricating biogenic silver nanoparticles (AgNPs) using an aqueous extract of *Catha edulis* (Qat; khat) leaves. The final product was characterized using various analytical techniques. Parameters' optimization including pH, contact time, temperature, and amount of leaf extract were carried out. AgNPs formation was confirmed by UV-vis spectra at 403 nm, FT-IR, and XRD peaks. FTIR spectra showed the presence of various biochemical metabolites which played a critical role in the bio-reduction, capping, and stabilization of AgNPs. The biogenic AgNPs were spherical in shape with an average size between 27 and 32 nm as estimated from XRD and SEM images. Biogenic AgNPs showed significant activities against sensitive and multi-drug resistance *Escherichia coli* and *Staphylococcus aureus* strains. In addition, the experimental results proved that AgNPs have higher efficacy than antifungal drugs that are commonly used to treat *Candida albicans* oral infections.

Keywords

Silver Nanoparticles, Biosynthesis, *Catha edulis*, *Candida albicans*, Antibacterial Activity

1. Introduction

Antibiotic resistance (ABR) is a global crisis that requires an international collaboration to minimize its impact on humanity. It has formidable health and economic consequences affecting individuals and health systems. According to recent estimations, the annual cost of ABR adds up to about 55 billion dollars in the USA and 9 Billion Euros in Europe [1]. Without proper intervention, the estimated economic burden due to ABR could reach 100 trillion US Dollars by 2050 [2] [3]. Health wise, the term post antibiotic era has emerged revealing a reality that bacteria and fungi are no longer affected by antibiotics [1] [4] [5]. Bacteria's natural adaptation to antibiotics has been developed due to the unnecessary exposure to sub-lethal quantities of drugs [2] [3] implying that a simple infection could be health threatening for many patients [6]. The mortality rate due to ABR pathogen infections could be as high as 50% [7] and by the year 2050, it is expected to cause more mortality than cancer to reach 10 million where Asia and Africa are impacted the most [1].

Antibiotic-resistant gram-negative *Escherichia coli* (*E. Coli*) and gram-positive *Staphylococcus aureus* (*S. aureus)* are among pathogens that have developed antibiotic-resistant strains. *E. coli* is the main threat of bloodstream infection in patients suffering from onco-haematology with the resistance level reaching 25.7% to third generation cephalosporins [8]. For patients with urinary tract infection, resistance of *E. coli* to at least one antibiotic reaches 45% and 60.9% for two examined antibiotics according to [9]. Alarmingly, *E. coli* resistance in animals and humans is recently reported against colistin antibiotic which is considered as one of the last chemical arsenal in man's defense against resistant pathogens [10] [11].

S. aureus is a gram-positive pathogen that causes serious skin and soft tissue infections and is considered one of the most commensal resistant drug pathogen worldwide [12] [13] [14] [15]. Although few options are still available for the treatment of infections caused by methicillin-resistant *S. aureus* (MRSA) [16], only two antibiotics are approved by Food and Drug Administration in the US [17].

Fungal infections caused by *Candida* species including *Candida albicans* are at the forefront of causing bloodstream infection with a mortality rate reaching 45% [5] [18].

Taking into consideration the fact that multi-drug resistant pathogens are a real threat to human, and the fact that pharmaceutical industries are reluctant to invest in the area of new antibiotics development [19], alternative approaches to cope with ABR challenge are a must. In recent years, attention has been shifted toward the development of nanoparticles (NP) and especially green synthesized silver nanoparticles (AgNPs). In this respect, various approaches have been successfully adapted for the biogenic synthesis of AgNPs including the use of bacteria, fungi, yeasts, algae, and plants. These unique nanotechnology procedures are advantageous due to development demand for environmental friendly technology for material synthesis. In addition, scientific reports reflect the unique prop-

erties AgNPs possess that find myriad applications such as antibacterial, antifungal, antivirus, and anticancer drugs, larvicidal excellent catalytic natural action towards degradation of dyes, very good antioxidants, treatment of diabetes-related complications, and wound healing activities [20] [21] [22] [23]. Moreover, antifungal impact of silver nanoparticles (AgNPs) was evaluated on the growth, morphological, and biomolecules dynamics of *Fusarium culmorum* and *Alternaria alternata.* It was revealed that the different concentrations of AgNPs caused inhibition of fungal growth and deformations of fungal structures especially at high concentrations 40 and 60 ppm of AgNPs. *A. alternata* conidiospores at 40 ppm of AgNPs were sharply deformed and their longitudinal sections disappeared. On the other hand, these fungi failed to produce conidiospores in the presence of 60 ppm of AgNPs but produced chlamydospores [24]-[29].

In this context, the present work aimed to optimize synthesis procedure for biogenic formation of AgNPs from aqueous extract of *Catha edulis* leaves. Antibacterial and antifungal efficacy of biogenic AgNPs were evaluated against resistant and sensitive *E. Coli* and *S. aureus* bacteria strains as well as resistant *Candida albicans* isolates.

2. Materials and Methods

2.1. Materials

2.1.1. Plant and Chemicals

The leaves of *Catha edulis Forsk* were purchased fresh from the khat market, Sana'a, Yemen, and the sample was further authenticated by the plant pharmacognosist at the Department of Pharmacognosy, Faculty of Pharmacy, University of Science and Technology (UST), Yemen. Silver nitrate ($AgNO_3$, 99%), Nutrient agar (NA), ciprofloxacin, vancomycin, nystatin (50 µg), itraconazole (30 µg), ketoconazole (30 µg) and fluconazole (10 µg) antibiotic disks standards were from HiMedia, India. Mueller-Hinton agar (MHA), Mueller-Hinton broth (MHB), H_2SO_4, copper acetate, ferric chloride, ninhydrin, HCl, KOH, iodine and potassium iodide were purchased from Sigma Aldrich. Sabourud dextrose agar was from Oxide, India. All chemicals were of analytical reagent grade and were used without further purification. Milli-Q water was prepared in-house and used in all experiments as needed.

2.1.2. Cultures

Standard cultures for antibacterial assays were obtained from the Hospital of University of Science and Technology, Sana'a, Yemen. These include Gram-positive *Staphylococcus aureus* sensitive and *methicillin-resistant S. aureus* (MRSA) and Gram-negative *Escherichia coli* sensitive and extended-spectrum *β*-lactamase-producing *E. coli* bacterial pathogens. As for *Candida Albicans*, a number of (5) isolates were obtained from patients of dental clinics in Taiz city, Yemen during the period from 1/10/2021 to 25/12/2021. Isolates were identified by specialists as *Candida Albicans.* Inform consent from each patient was obtained according to the guidelines of the Taiz University Ethics Committee.

2.2. Methods

2.2.1. Preparation of *Catha edulis* Leaves Extract

Fresh leaves of *Catha edulis* were washed with running tap water and then with Milli-Q water to remove dirt, soil, and undesirable particles. Then the leaves were dried at room temperature for 15 minutes to remove the water from the surface of the leaves. About 25 g of plant's leaves were boiled in 100 mL of deionized water at 70˚C for about 30 min. The boiled water with the leaves was centrifuged for 10 min at 9000 rpm and filtered using Whatman filter paper to produce clear extraction solution. Then the extract was stored at 4˚C - 8˚C and used as reducing as well as stabilizing/capping agent.

2.2.2. Determination of the Phytochemical Constituents

Examination of the biologically active constituents (alkaloids, tannins, flavonoids, phenols, saponins, proteins, carbohydrates and terpenes) in the aqueous extract of *Catha edulis* leaves was carried out using standard biochemical methods as described by [30] [31] [32].

2.2.3. Procedure Optimization for the Biosynthesis of AgNPs

Reaction parameters that could possibly affect the rate of biosynthesis and alter the AgNPs shape and morphology were optimized. The optimization process was performed by changing one factor and keeping the rest constant.

1) Optimization of the Reactants Ratio, Time, Temperature, and pH

Different ratios in mL (1:99, 5:95, 10:90 and 15:85) of aqueous extract and 1 mM $AgNO_3$ respectively were used to find out the optimum values. Experiments were performed at room temp (25˚C) and caution was taken to prevent photoactivation of silver nitrate via keeping the reactants in the dark for the specified testing time.

Reaction time was monitored at a different time for 48 hrs, by recording visual observations and UV-visible spectra of the formed AgNPs. The effect of temperature on the biosynthesis of AgNPs was also examined at different temperatures (10˚C, 30˚C, 50˚C, and 70˚C) via monitoring the UV-visible spectra of the AgNPs solutions for 24 h/sample.

The pH effect on the formation of AgNPs was examined at various pH (5.0, 7.0, 8.0 and 9.0) using reactants optimal ratio 1:99 (leaves extract: 1 mM $AgNO_3$) and 70˚C. The solution acidity was adjusted using 0.1 N KOH or 0.1 N HCl as needed.

2.3. Silver Nanoparticles Biosynthesis under Optimized Conditions

The synthesis step was done as follows: A volume of 99 mL (1 mM $AgNO_3$) was transferred to 250 mL Erlenmeyer flask followed by the addition of 1 mL aqueous leaves extract using a sterilized syringe with small needle. The solution's acidity was adjusted to pH 9. The flask was covered with aluminum foil and placed on a hot plate whose temperature was maintained at 70˚C. The content was vigorously agitated with a magnetic stirrer for 24 h. Visual observations and UV-visible spectra of the solution were monitored and recorded.

2.4. Characterization of AgNPs

Formation of AgNPs was confirmed by recording the absorbance spectra using UV-visible spectroscopy (Analytical Jena-Specord 205, Germany) between 190 nm and 750 nm. Fourier Transform Infrared Spectroscopy (FTIR) was performed on (Perkin Elmer Spectrum 2, USA) to detect the possible functional groups of biologically active constituents present in the extract. The X-ray diffraction (XRD) measurements were performed on X-ray diffractometer (Bruker AXS, Germany) operated at 10 kV and spectrum was recorded with wavelength of 1.5406 Å in the 2θ range of 20˚ to 80˚. The surface morphology and size of the AgNPs were scanned using a scanning electron microscope (SEM) on (JEOL, Tokyo, Japan).

2.5. Antibacterial Activity of AgNPs

The assessment of antibacterial activities of AgNPs was carried out in a laminar flow cabinet with standard sterile conditions using a procedure that was described in previous studies [33] [34]. In summary, the gram-negative (*E. coli*) and gram-positive (*S aureus*) bacterial cultures were prepared by the standard process. The petri-dish and agar were autoclaved before use. Leaf extract and silver nanoparticle samples were exposed to UV radiations for 1 h to remove any unwanted bacterial impurity. Pure bacterial (a single colony) cultures were uniformly spread on nutrient agar plates using L-rod glass. Leaf extract, AgNPs and silver nitrate were transferred to sterilized filter paper (Whatman. No 1, 6 mm in diameter) discs, which subsequently were air-dried under sterile conditions. Using sterile forceps, the dry paper discs were placed on the MH agar plate and were left for 30 min for compound diffusion at room temperature. Vancomycin and ciprofloxacin were used as positive controls for Gram-positive *Staphylococcus aureus* and Gram-negative *Escherichia coli* bacteria, respectively. The plates were incubated at 37˚C for 24 hrs. Finally, the maximum zone of inhibition against each type of tested microorganism was measured in triplicate.

2.6. Antifungal Activity

Anticandidal activities of AgNPs, $AgNO_3$, *Catha edulis* extract and standards antibiotics against five different *C. albicans* strains were determined using disk diffusion method according to the guidelines of Clinical and Laboratory Standards Institute (CLSI) for bacteria and yeasts testing [35].

In brief, a bacterial suspension was made and adjusted to 0.5% McFarland $BaSO_4$ standard (1.5×10^8 colony-forming unit/mL). A sterilized cotton swap was used to spread the standard suspension on the petri dish containing Sabourud dextrose agar (SDA) for culturing the pathogenic fungi. Individual sterile filter papers were made from (Whitman No 1). Each piece was soaked in either 100 or 150 µg/disc of AgNPs, $AgNO_3$, *Catha edulis* leaves extract. Disks were placed on medium containing fungi and incubated at a temperature of 37˚C for 48 hours. The results were monitored for three days. The inhibition zones were measured in mm and the results were recorded.

3. Results and Discussion

3.1. Phytochemical Screening Tests and pH Value of the Aqueous Extract

The results of qualitative phytochemical screening and pH value of aqueous extract of *Catha edulis* leaves were shown in **Table 1**. The obtained data revealed the presence of alkaloids, flavonoids, phenols, tannins, saponins, carbohydrates, and terpenes. The pH value (7.33 ± 0.20) confirmed the availability of some basic active constituents in the extract such as the phenylpropylamino alkaloids, cathinone (aminopropiophenone), cathine and norephedrine. Our results were in-line with data reported previously [36].

3.2. Silver Nanoparticles Biosynthesis under Optimized Conditions

After the addition of leaf aqueous extract to the solution containing 1 mM $AgNO_3$ under optimized reaction condition (temperature, pH, reactants ration and time), deep reddish-purple color was observed with λ_{max} = 403 nm as shown in **Figure 1** confirming the synthesis of AgNPs, compared to no color change observed in the absence of plant extract. These results agreed well with the results of previous studies [37] [38]. Kumar and Kathireswari, suggested that color change is due to the excitation of surface plasmon resonance (SPR) of AgNPs which results from the reduction of Ag^+ to Ag^0 by the biologically active constituents of the leaves aqueous extract. In addition, these constituents act also as stabilizing agents for the AgNPs [39] [40]. The location of SPR wave-length below 450 nm for the deep reddish-purple solution may indicate the formation of spherical AgNPs as suggested by previous researcher [41]. The appearance of a single SPR band in the absorption spectrum is a confirmation of spherical nanoparticles [42] [43]. Moreover, with increasing the time of incubation "**Figure 2**", there was an increase in the absorbance intensity without any additional blue shift

Table 1. Phytochemical screening and pH value of *Catha edulis* leaf extract.

S. no.	Phytochemicals	*Catha edulis*
1	Alkaloids	+
2	Tannins	+
3	Flavonoids	+
4	Phenols	+
5	Saponins	+
6	Proteins	–
7	Carbohydrates	+
8	Terpenes	+
9	pH	7.33 ± 0.2

+ sign indicates positive test and – sign indicates negative test.

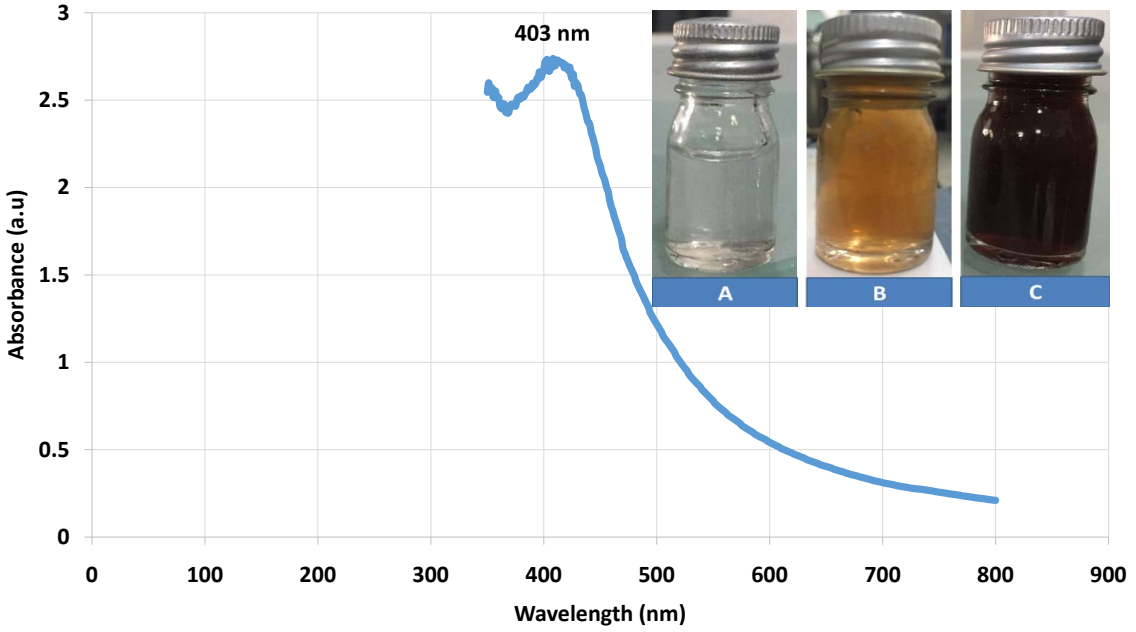

Figure 1. UV-Vis spectra and visual observation of silver nanoparticles (AgNPs) synthesized under optimized conditions. (A) 1 mM $AgNO_3$; (B) *Catha edulis* leaf extract; (C) AgNPs.

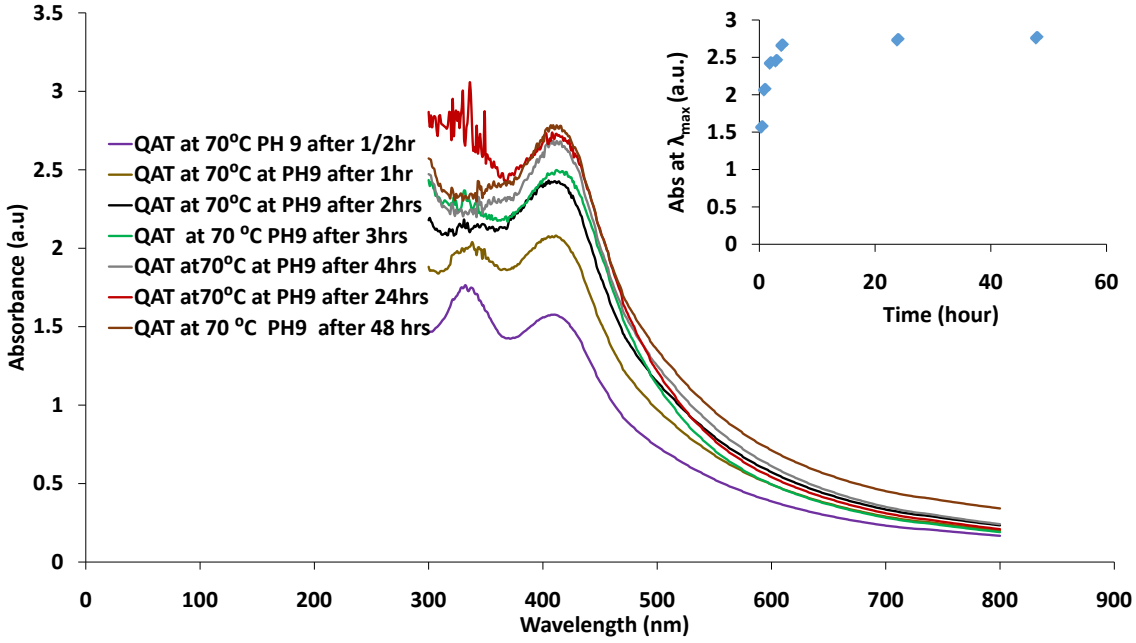

Figure 2. UV-Vis spectra of silver nanoparticles (AgNPs) synthesized under optimized conditions at different durations.

in λ_{max} indicating a complete reduction of silver ions after 24 h. Similar observation was reported by other investigators [34] [44] [45] [46].

The biosynthesis of AgNPs at optimum reaction conditions was favorable due to higher kinetic energy and surface charges of the biologically active constituents. This resulted in faster Ag^+ reduction and deposition of the biological constituents on the surface of the AgNPs leading to less aggregation of the nanoparticles.

3.3. Parameters' Optimization for the Biosynthesis of AgNPs

3.3.1. Effect of Reactants Ratio and Reaction Time on Biosynthesis of AgNPs

Photographic observation shown in Figure 3 revealed that the reduction of Ag^{+} to Ag^{0} was occurred, and the process was dependent on the reactants' ratio. The optimum ratio of *Catha edulis* aqueous extract to that of $AgNO_3$ was 1:99 (v/v). This was confirmed by the UV-visible spectra "Figure 4" which showed that the highest peak was produced when the aforementioned ratio (1:99) was used. In the cases when the extract volume was increased, the observed color change of

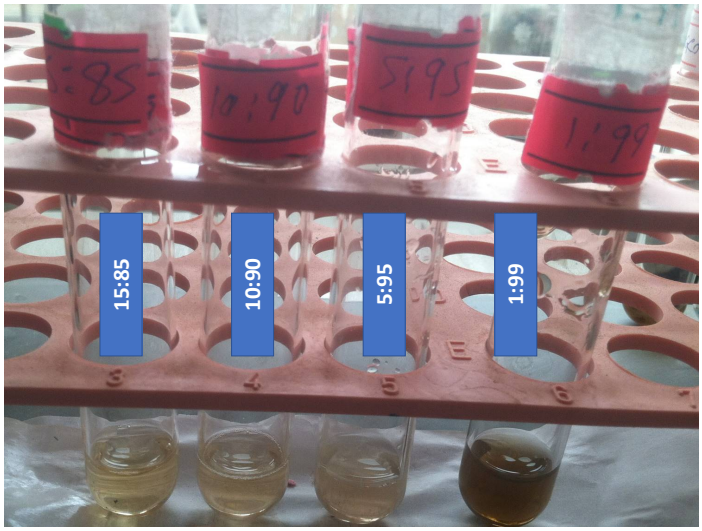

Figure 3. Color change for AgNPs synthesized at room temperature with different ratios of leaf extract and 1 mM $AgNO_3$ after 24 hrs.

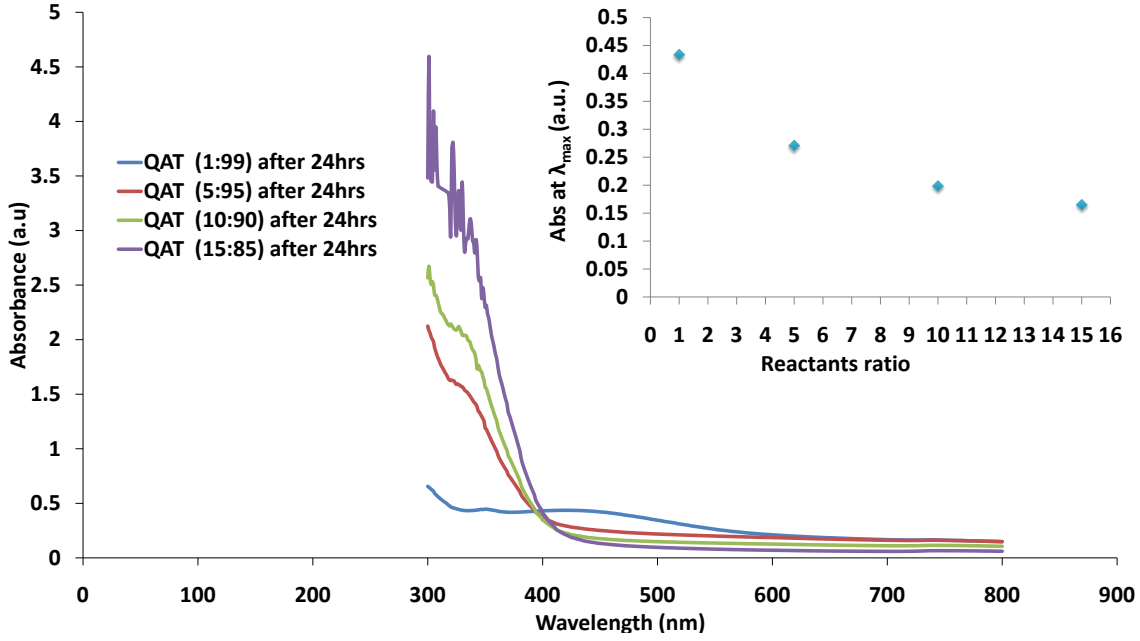

Figure 4. UV-Vis spectra of silver nanoparticles (AgNPs) synthesized at room temperature with different ratios of leaf extract and 1 mM $AgNO_3$ after 24 hrs.

the solution was less intense and the absorption was decreased, which may be attributed to the production of biosynthesized silver nanoparticles with large size particles. On the other hand, when the extract volume was less than the optimal value (*i.e.* the biologically active constituents were lower), the chances of silver nanoparticles formation were less, and therefore the absorption intensity was decreased. Similar observation was reported earlier [47].

The effect of contact time between silver nitrate and *Catha edulis* aqueous extract on the formation AgNPs was also investigated at room temperature. Results shown in **Figure 5** indicated that the absorption intensity of the UV-Vis band increased with increasing incubation time. Furthermore, when the incubation time was less than 1 h, the AgNPs were not formed. Our results were in-line with those reported by [20] [47] [48].

3.3.2. Effect of Temperature

Temperature is an important factor with a significant effect on biosynthesis of AgNPs. Data in **Figure 6** suggested that the optimum temperature for the synthesis of AgNPs was 70˚C. As the reaction temperature increased from 10˚C to 70˚C, the rate of the reduction process of Ag^{+} to Ag^{0} went up due to increasing the kinetic energy of biologically active constituents. The rapid change and more intense color formation at higher temperature was noticed, which was associated with blue shift, narrow peaks and higher absorption intensity of the UV-Vis spectra indicating the production of higher amount of AgNPs with smaller particle size. Our observations were in agreement with the results of previous studies [47] [48] [49]. On the contrary, the UV-Vis spectrum at lower temperature had a broader UV-Vis absorption band, which could be ascribed to the formation of large size AgNPs as suggested previously [50].

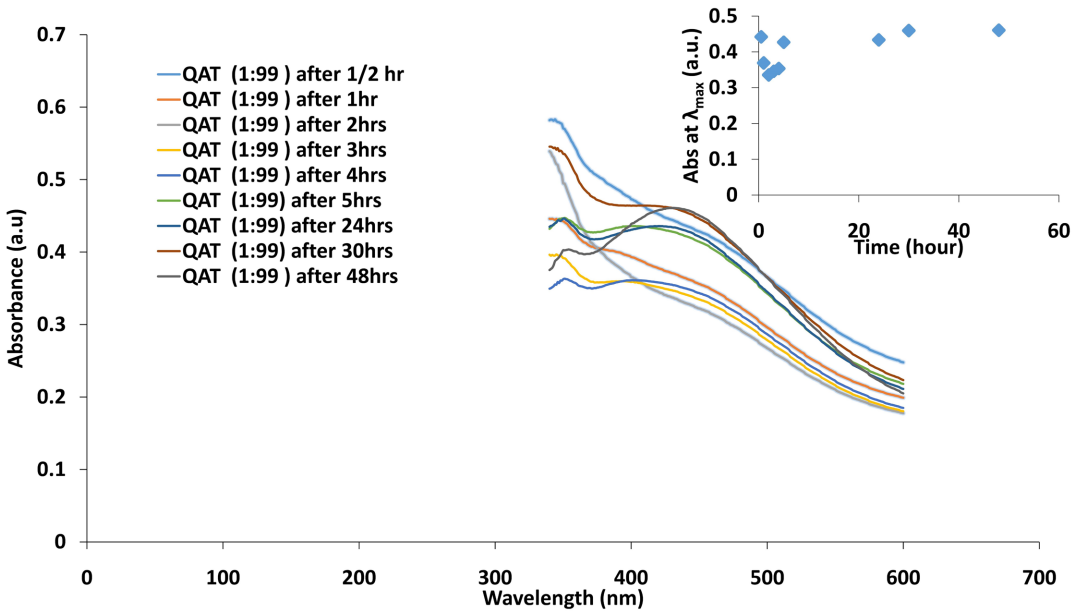

Figure 5. UV-Vis spectra of silver nanoparticles (AgNPs) synthesized at room temperature using (1:99) ratio of leaf extract and 1 mM $AgNO_3$ observed at different reaction times.

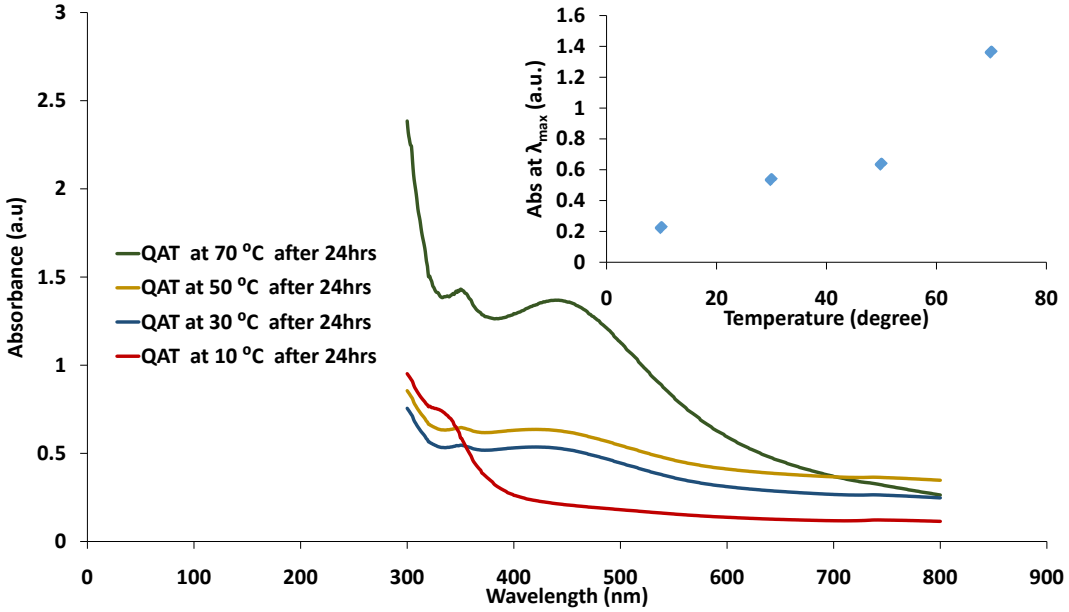

Figure 6. UV-Vis spectra of silver nanoparticles (AgNPs) synthesized at 10˚, 30˚, 50˚, and 70˚C using (1:99) ratio of leaf extract and 1 mM $AgNO_3$ after 24 hrs.

3.3.3. Effect of pH

Another important parameter is the pH, which affects the AgNPs biosynthesis. **Figure 7** suggested that pH 9.0 was found to be the most favorable medium for the biosynthesis of AgNPs, where the blue shift was also observed. The λ_{max} was recorded at 403 nm, indicating the formation of smaller size of AgNPs. Moreover, the results showed that increasing reaction medium pH from acidic (pH 5.0) to alkaline (pH 9.0) resulted in improving the rate of bioreduction process of Ag^+ possibly due to forming more negative ionizable groups of the natural biologically active constituents present in the extract. This was also suggested by the rapid increase in the color intensity of the reaction solution and the UV-vis absorption peak at alkaline pH. Similar results were reported in the literature [50] [51] [52]. Acidic pH tends to cause nucleation and form large particles size as noted by [34].

3.3.4. FTIR Spectroscopy

FTIR spectra of the *Catha edulis* leaf extract and biosynthesized AgNPs were shown in **Figure 8**. The spectrum of the leaf extract "**Figure 8(A)**" exhibited a strong band at 3368.69 assigned to OH^- stretching alcohol group. This band experienced a significant decrease in its intensity and a large shift toward higher wavenumber (3410.56 cm^{-1}) in the spectrum of AgNPs "**Figure 8(B)**" indicating the binding of silver ions with hydroxyl groups of phenolic compounds, flavonoids, terpenoids and carbohydrate present in leaf extract [34] [53]. Both spectra showed a band at 2930.7 cm^{-1} assigned to C-H vibration mode. A prominent band (1622.91 cm^{-1}) in the spectrum of the leaf extract that could be attributed to stretching of amide I [53] or vibration of cyclobenzene [54] exhibited a shift toward lower wavenumber (1610.81 cm^{-1}) and major decrease in the absorption

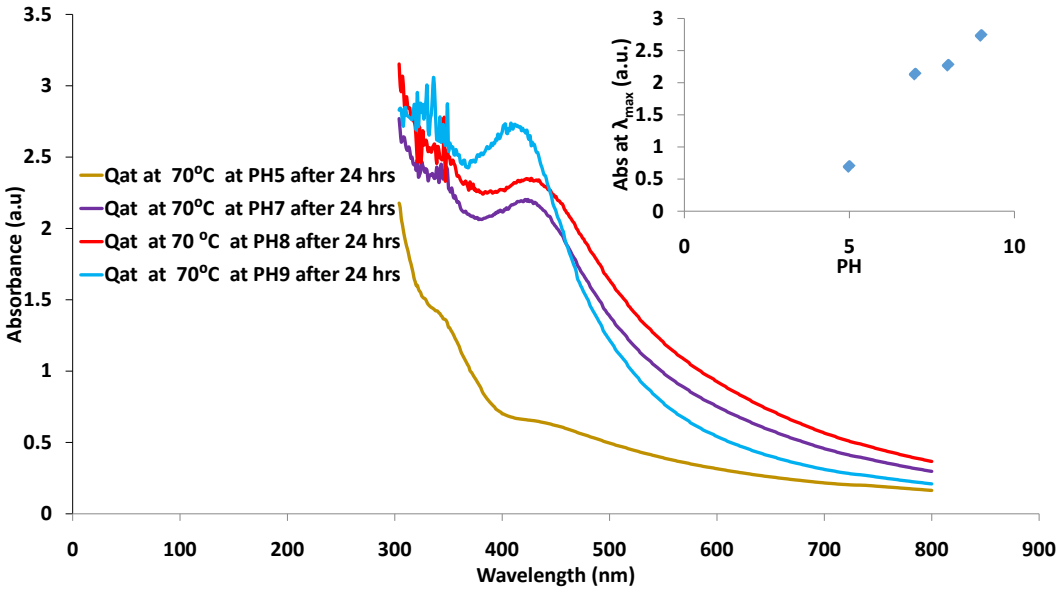

Figure 7. UV-Vis spectra of silver nanoparticles (AgNPs) synthesized at 70˚C, at various pH (5.0, 7.0, 8.0 and 9.0) using (1:99) ratio of leaf extract and 1 mM $AgNO_3$ after 24 hrs.

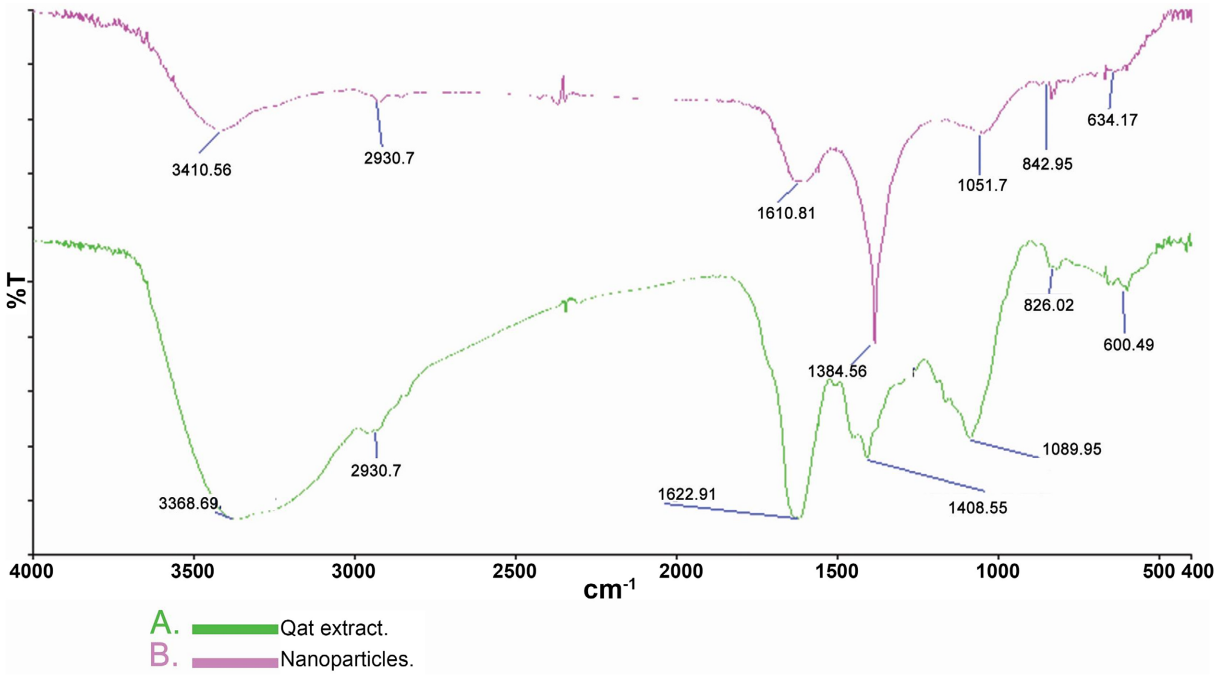

Figure 8. FTIR spectrum. (A) FTIR of *Catha edulis* A. leaf extract; (B) FTIR of AgNPs synthesized.

intensity indicating the interaction of this group with AgNPs. The shift in (C-O) absorbance band from 1408.55 cm^{-1} (leaf extract) to 1384.56 cm^{-1} (AgNPs) was attributed to the coordination of the silver ions with carboxylate [42] [53]. The change in the position of (C-N) band from 1089.95 cm^{-1} (leaf extract) to 1051.7 cm^{-1} (AgNPs), indicates the involvement of aliphatic amine in the formation of silver nanoparticles [42] [53]. The peak observed at 842.95 cm^{-1} (AgNPs) was attributed to the bending vibrations of C-H groups of phenyl rings [55]. The fi-

nal shift in absorption peak from 600.49, (leaf extract) to 634.17 cm^{-1} (AgNPs) indicated the bonding between silver nanoparticles and the oxygen of hydroxyl groups [42]. FTIR spectroscopy confirmed that the active constituents of the leaf extract such as flavonoids, terpenoids, and carbohydrates had a major role in the formation of AgNPs via transformation mechanism from enol to keto form [56] [57] [58]. The abundance of -OH groups present in quercetin, for example, may be responsible for releasing reactive hydrogen atoms that reduce silver ions to AgNPs [59] [60].

3.3.5. X-Ray Diffraction (XRD)

The XRD analysis was done to figure out the crystalline nature of the AgNPs. The XRD pattern showed many distinct peaks at approximately 38.20˚, 45.50˚, 64.60˚ and 77.38˚ corresponding to (111), (200), (220), and (311) planes of silver metal respectively "**Figure 9**".

These peaks indicated the crystalline face-centered-cubic (fcc) nature of the AgNPs and are in agreement with the database of the Joint Committee on Powder Diffraction Standards (JCPDS No. 04-0783). The XRD peaks revealed that the synthesized silver nanoparticles were spherical and crystalline in nature [49] [61]. Additional peaks were also observed at 27.42˚, 44.36˚, 56.56˚, 66.44˚, and 75. 34˚; may be due to organic constituents that were present in the extract and responsible for silver ions reduction and stabilization of resultant nanoparticles. Using Debye-Scherrer Equation [51], the calculated average crystallite of the AgNPs were ~27 nm.

3.3.6. Scanning Electron Microscopy (SEM)

For additional confirmation of the size and shape of the biosynthesized AgNPs, SEM analysis was carried out. **Figure 10** confirmed the biosynthesis of spherical

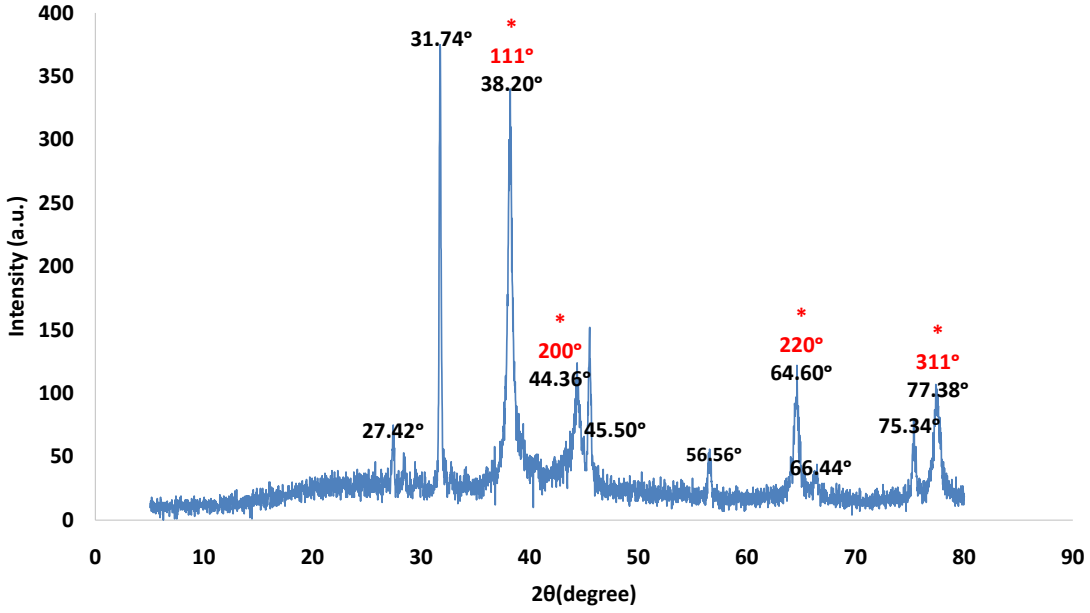

Figure 9. XRD pattern of biofabricated AgNPs.

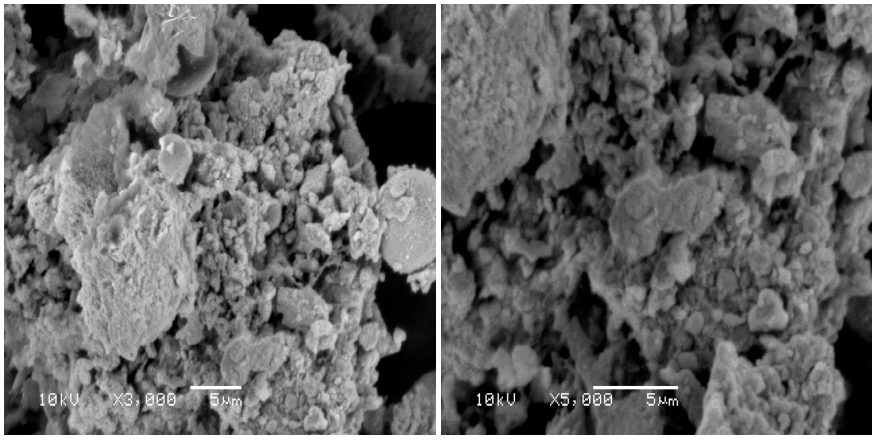

Figure 10. SEM images of Silver Nanoparticles (AgNPs) synthesized using *Catha edulis* aqueous extract.

particles shape with average size 32 nm. This result confirmed our UV-Vis data where a single sharp peak was seen indicating the formation of smaller particles. AgNPs showed some agglomeration that could be attributed to the presence of bio-reducing and capping agents of *Catha edulis* aqueous extract around and on the surface of the biosynthesized AgNPs [45] [50] [62].

3.3.7. Antimicrobial Activity of AgNPs against Pathogenic Antibiotic Sensitive Bacteria

The bio-fabricated silver nanoparticles using *Catha edulis* aqueous extract were evaluated for their antibacterial activity using selected pathogenic bacteria which were sensitive to vancomycin and ciprofloxacin antibiotics. In the current work, the inhibition zones caused by AgNPs, silver nitrate and leaf extract disks were noted and measured after 24 hours of incubation at 37˚C. Mariselvam *et al*., suggested that zones with diameters of <9 mm were considered as inactive, 9 - 12 mm as moderately active, and 13 - 18 mm as active [63]. Antimicrobial activities of AgNPs samples (100 µg/disc and 150 µg/disc) shown in **Table 2**, **Figure 11**, and **Figure 12** against human pathogenic antibiotic-sensitive bacteria revealed that the AgNPs have a moderately active antimicrobial activity against both S. *aureus* and *E. coli* sensitive strains that reached 13.2 ± 0.3 and 14.0 ± 0.5 mm respectively. Higher inhibition zones were observed with increasing AgNPs concentration to reach 18.3 ± 0.57 and 20.0 ± 0.5 mm. The antibacterial activities of AgNPs are relatively good compared to those observed with standard 30 µg/disc vancomycin and 5 µg ciprofloxacin antibiotics. Our results were in line with those reported in the literature [33] [38] [64] [65]. Interestingly, the aqueous leaf extract did not show observable antibacterial activities against both −ve and +ve sensitive bacterial strains, while Ag^{+} activity was about 50% of that exhibited by the AgNPs. Shanmuganathan et.al attributed that to the high areas-to-volume ratio of the AgNPs that enable them to penetrate the bacteria cell walls and cause the death of bacteria as a final result via various proposed mechanisms [66].

Table 2. Antibacterial activities of 100 µg/disc and 150 µg/disc of AgNPs, $AgNO_3$, *Catha edulis* leaf extract, and reference antibiotic drugs (ciprofloxacin and vancomycin) against *E. coli* and *S. aureus* pathogenic antibiotic sensitive bacteria.

Conc. of AgNPs	Pathogenic species	Mean zone of inhibition (mm ± SD)				
		AgNPs	$AgNO_3$	Leaf extract	Vancomycin 30 µg	Ciprofloxacin 5 µg
100 µg/disc	*S. aureus*	13.2 ± 0.3	7.0 ± 0.2	NA[a]	27.0 ± 0.0	
	E. coli	14.0 ± 0.5	7.0 ± 0.4	NA[a]		30.0 ± 0.0
150 µg/disc	*S. aureus*	18.3 ± 0.3	9.2 ± 0.57	NA[a]	27.0 ± 0.0	
	E. coli	20.0 ± 0.5	9.5 ± 0.5	NA[a]		30.0 ± 0.0

NA[a] represents poor antibacterial activity.

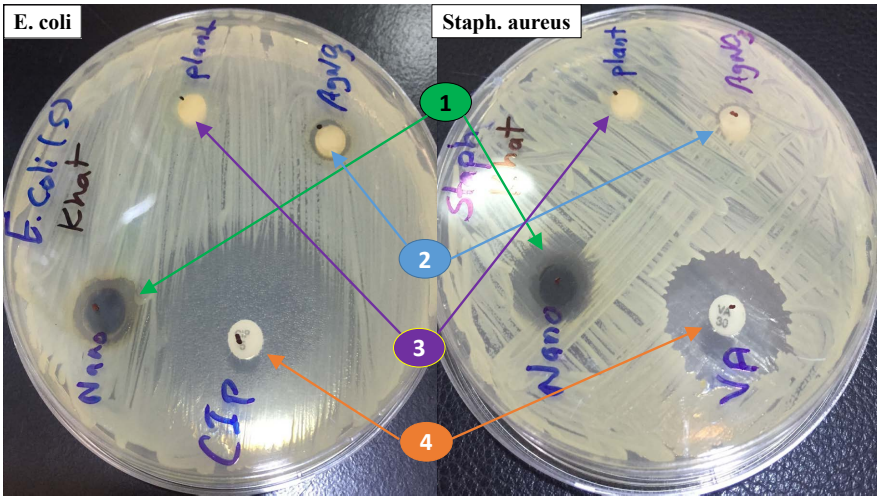

(A)

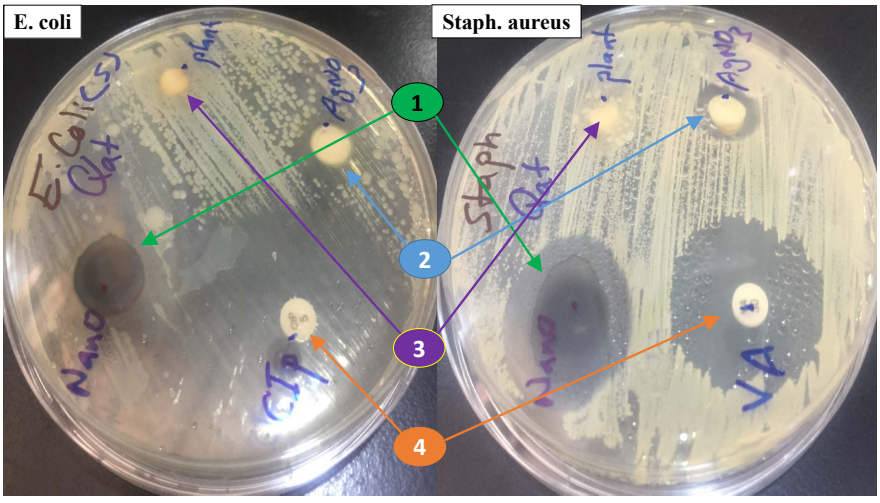

(B)

Figure 11. The antibacterial activity of (1) AgNPs; (2) $AgNO_3$; (3) *Catha edulis*; (4) Standard reference antibiotic drugs (ciprofloxacin and vancomycin) against *E. coli and S. aureus* pathogenic antibiotic sensitive bacteria (A) 100 µg/disc and (B) 150 µg/disc of AgNPs.

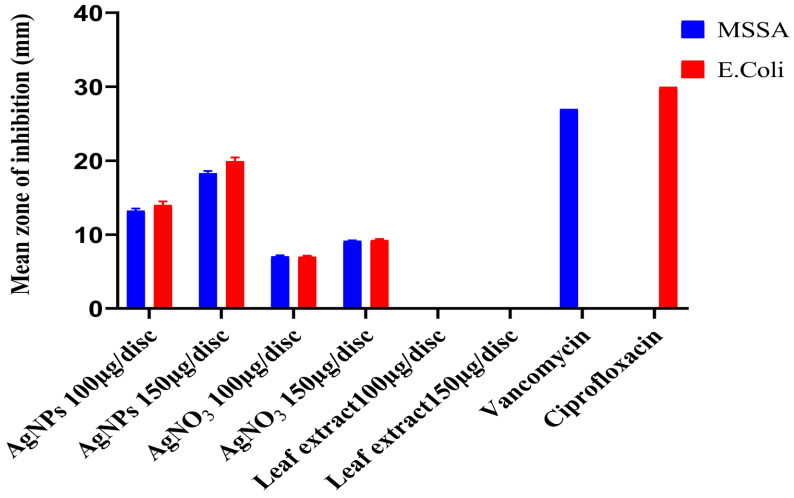

Figure 12. The antibacterial activity of AgNPs, $AgNO_3$, *Catha edulis*, and Standard reference antibiotic drugs (ciprofloxacin and vancomycin) against *E. coli* and *S. aureus* (MSSA) pathogenic antibiotic sensitive bacteria using two different concentrations of AgNPs (100 and 150 µg/disc).

3.3.8. Antimicrobial Activity of AgNPs against Pathogenic Antibiotic Resistance Bacteria

The antimicrobial efficacy of bio-fabricated AgNPs was investigated against two antibiotic-resistant bacteria strains namely methicillin-resistant *S. aureus* (MRSA) and extended-spectrum *β*-lactamase-producing *E. coli* bacteria. Two different concentrations (100 and 150 µg/disc) of AgNPs were used and their antibacterial activities were compared to those of Ag^+, *catha edulis* aqueous extract, and antibiotic standards as shown in **Table 3**, **Figure 13**, and **Figure 14**. Few observations could be made from these findings. First, *E. coli* Gram −ve bacteria is totally resistant to antibiotic ciprofloxacin standard at a concentration of 5 µg while Gram +ve *S. aureus* exhibits a moderate resistivity against vancomycin (30 µg) antibiotic standard. The inhibition zone of standard vancomycin which is considered the drug of choice to treat *S. aureus* bacterial infection reached only 14 ± 0 mm. Second, AgNPs showed moderate inhibition against both resistant bacteria strains. The inhibition efficacy increased with increasing concentration and even exceed the inhibition activity of standard vancomycin antibiotic. This finding confirms previous results of the high potentials of using AgNPs as an alternative therapeutic strategy to tackle the wide spread of antibiotic-resistant bacteria infections [21] [22] [67]. Third, leaf aqueous extracts of *Catha edulis* and silver ions apparently were inactive against both resistant bacteria strains according to the classification of [63]. Fourth, the inhibition zone was higher for the Gram-negative bacteria (*E. coli*) compared to that of Gram-positive bacteria (*S. aureus*). The difference in sensitivity may be attributed to the variation in the cell membrane structure. Cell membrane of Gram-negative bacteria is covered by peptidoglycan as single layer, whereas cell membrane of Gram-positive bacteria is covered by peptidoglycan as multi-layers that make the cell more rigid for nano particle penetration.

Table 3. Antibacterial activities of 100 µg/disc and 150 µg/disc of AgNPs, $AgNO_3$, *Catha edulis* leaf extract, and reference antibiotic drugs (ciprofloxacin and vancomycin) against *E. coli* and *S. aureus* pathogenic antibiotic-resistant bacteria.

Conc. of AgNPs	Pathogenic species	Mean zone of inhibition (mm ± SD)				
		AgNPs	$AgNO_3$	Leaf extract	Vancomycin 30 µg	Ciprofloxacin 5 µg
100 µg/disc	*S. aureus*	11.2 ± 0.57	7.0 ± 0.2	NA[a]	14.0 ± 0.0	
	E. coli	12.0 ± 0.5	7.0 ± 0.4	NA[a]		NA[a]
150 µg/disc	*S. aureus*	15.0 ± 0.5	9.5 ± 0.5	NA[a]	14.0 ± 0.0	
	E. coli	16.0 ± 0.6	9.5 ± 0.5	NA[a]		NA[a]

NA[a] represents poor antibacterial activity.

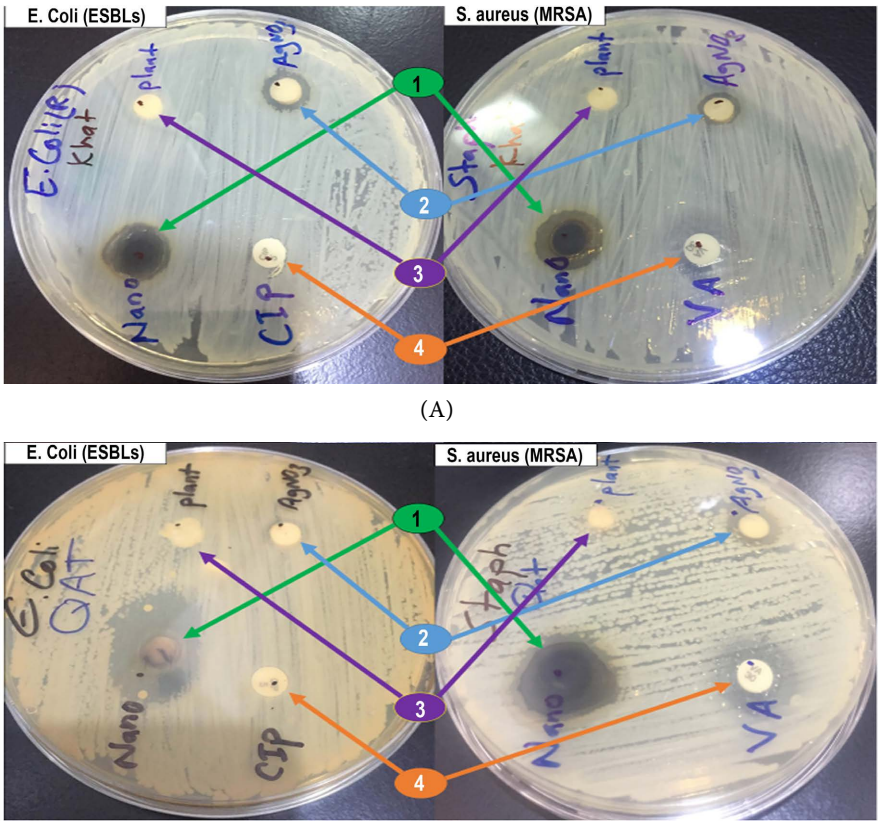

(A)

(B)

Figure 13. The antibacterial activity of (1) AgNPs; (2) $AgNO_3$; (3) *Catha edulis*; (4) Antibiotic drugs (ciprofloxacin and vancomycin) against *E. coli and S. aureus* pathogenic antibiotic resistance bacteria (A) 100 µg/disc and (B) 150 µg/disc of AgNPs resistance bacteria.

3.3.9. Antifungal Activity of AgNPs against *C. albicans*

Antifungal efficacy of AgNPs against *Candida albicans* was examined on five different isolates and the results were compared with those of standard antibiotics (nystatin 50 µg, itraconazole 30 µg, ketoconazole 30 µg and fluconazole 10 µg), *Catha edulis* extract and $AgNO_3$. The results were presented in **Figures 15(a)-(e)**

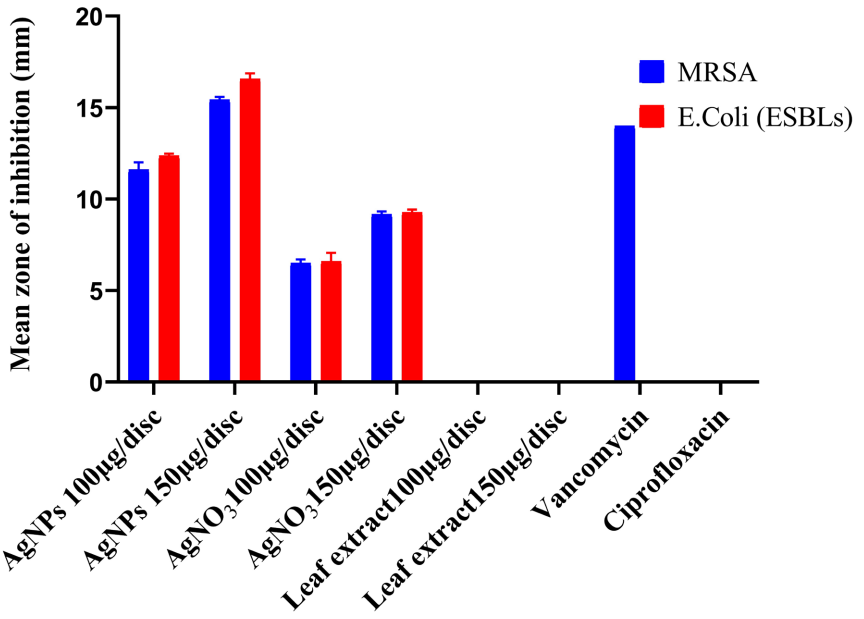

Figure 14. The antibacterial activity of AgNPs, $AgNO_3$, *Catha edulis*, and Standard reference antibiotic drugs (ciprofloxacin and vancomycin) against *E. coli* (ESBLs) and *S. aureus* (MRSA) pathogenic antibiotic resistance bacteria using two different concentrations of AgNPs (100 and 150 µg/disc).

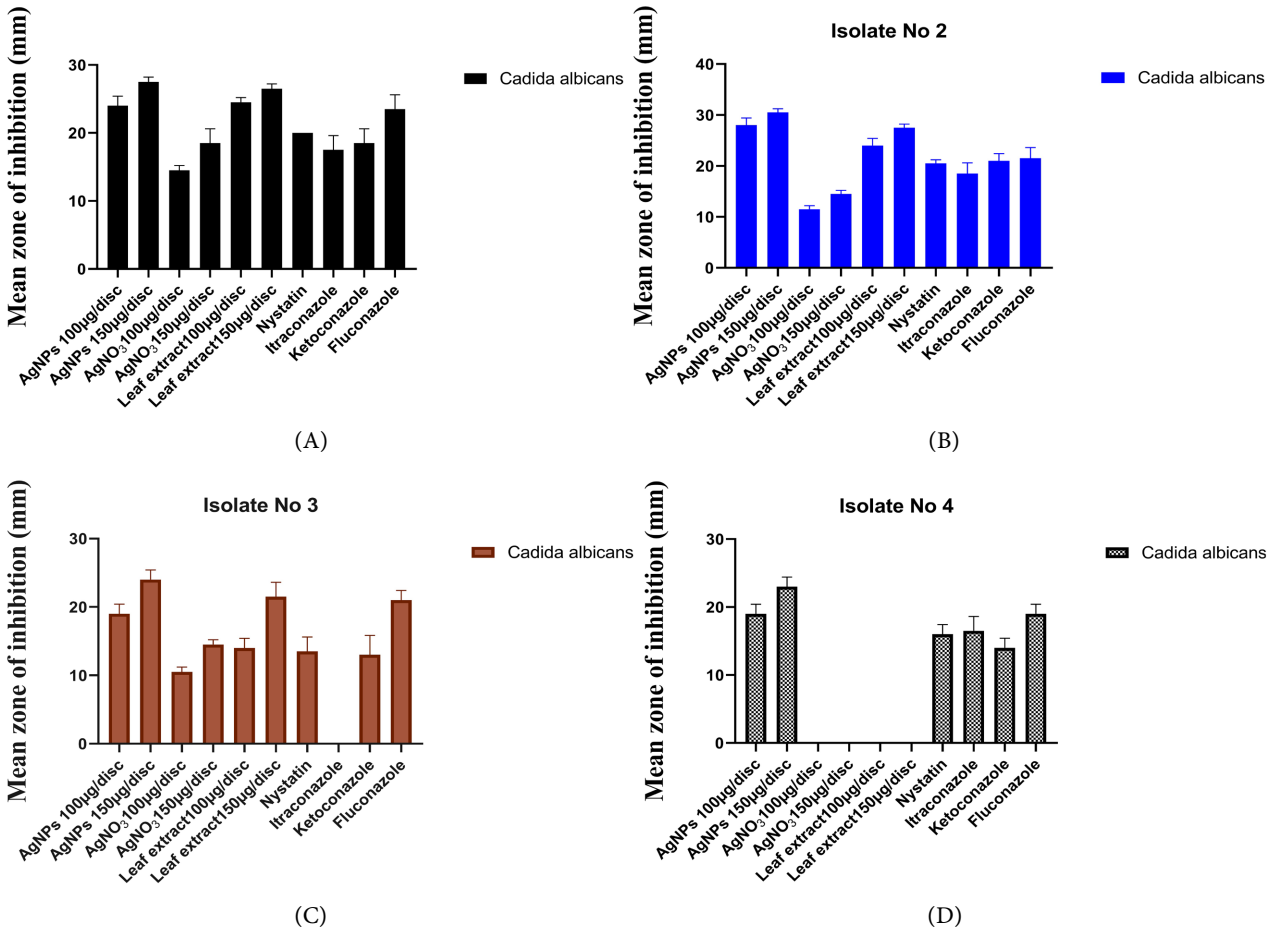

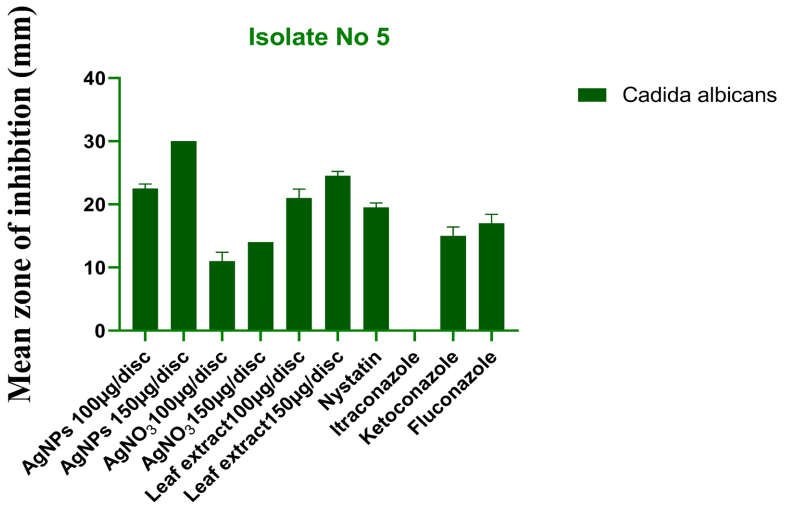

(E)

Figure 15. The antifungal activity of AgNPs, $AgNO_3$, *Catha edulis*, and antibiotic drugs (nystatin 50 µg, itraconazole 30 µg, ketoconazole 30 µg and fluconazole 10 µg) against *C. albicans*. (A) Isolate 1; (B) Isolate 2; (C) Isolate 3; (D) Isolate 4; (E) Isolate 5. AgNPs, leaves extract and $AgNO_3$ were used at two different concentrations (100 and 150 µg/disc).

and **Figure 16**. It could be inferred from these data that AgNPs exhibited excellent anticandidal activity against all isolates exceeding the efficacy of the four standard antibiotics which are considered among the drug of choice to tackle *Candida albicans* infections. The antifungal activity of AgNPs is a concentration dependent where the inhibition zones were larger when 150 µg/disc was used compared to 100 µg/disc AgNPs solution. This finding was in agreement with the work of Paul *et al.* [68].

Furthermore, the degree of anticandidal activity of AgNPs varied from one isolate to another. This was expected since the five isolates were taken from five different patients who possibly had developed different degrees of antibiotic resistance. This observation was also seen for antibiotics, $AgNO_3$ and leaf extract. For instance, all substances exhibited anticandidal activity against *Candida albicans* in isolates 1 and 2 to various degrees, while only AgNPs and standard antibiotics had antifungal activity in isolate 4. On the other hand, itraconazole had antifungal activity only against three out of five isolates. Interestingly, *Catha edulis* extract inhibited *Candida albicans* in four isolates out five. Plants species in general have developed a unique defense system against pathogenic infections via the development of secondary metabolites [69]. Saponin compounds which were tested positively in *Catha edulis* extract in our work were previously reported to have antimicrobial activity [70].

The antibiotic resistance is a result of the natural adaptation and unique mechanism developed by bacteria and fungi against antibiotics. Thus, nanoparticles and more specifically AgNPs could be alternative and successful therapeutic antimicrobial agents due to their chemistry, physical and morphology. These agents have a direct attachment to the cell wall of the invasive bacteria and fungi and in this way, pathogens may have less chance to develop ABR [69].

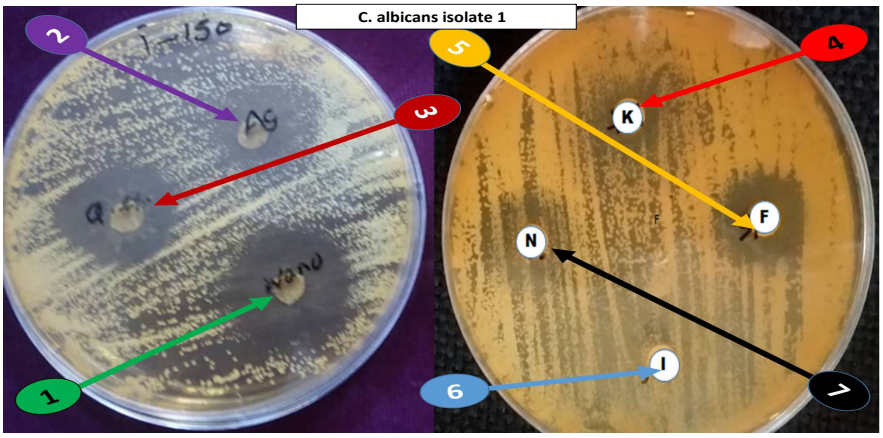

Figure 16. Representative anticandidal activity of (1) AgNPs; (2) $AgNO_3$; (3) *Catha edulis extract*; (4) Ketoconazole; (5) Fluconazole; (6) Itraconazole; (7) Nystatin against *C. albicans* in isolate 1. The concentrations of AgNPs, Silver ions and leaves extract were 150 µg/disc, while the concentrations of antibiotics were the same as shown in **Figure 15**.

4. Conclusion

AgNPs have been successfully biosynthesized using *Catha edulis* aqueous extract. The formation of AgNPs was critically dependent on the concentration of leaf extract, reaction time, pH and temperature which affected the size, and shape of the AgNPs. The biosynthesized AgNPs exhibited a high energy SPR band at 403 nm, as indicated by UV-Vis spectroscopy. Analytical techniques revealed that AgNPs were spherically shaped and crystalline in nature with an average diameter between 27 and 32 nm. AgNPs showed significant antimicrobial activities against pathogenic sensitive and resistant strains of *S. aureus* and *E. coli* as well as *Candia albicans* which exceeded that of the standard antibiotics, *Catha edulis* extract and $AgNO_3$. It is highly anticipated that biogenic metallic NPs could be viable and economical alternatives for treating drug resistant bacterial and fungi infections and deserve further clinal investigation.

Acknowledgements

The authors are thankful to the University of Science and Technology (UST), Faculty of Pharmaceutical Sciences and Central for Research and Pharmaceutical Studies (CRPS), Sana'a, Yemen.

Ethical Approval

The anti-fungal study was approved by the Ethics Committee for Scientific Research, Faculty of Medicine and Health Sciences, Taiz University, Taiz, Yemen.

Conflicts of Interest

The authors have not declared any conflict of interest.

References

[1] Dadgostar, P. (2019) Antimicrobial Resistance: Implications and Costs. *Infection*

and Drug Resistance, **12**, 3903-3910. https://doi.org/10.2147/IDR.S234610

[2] Roope, L.S., *et al.* (2019) The Challenge of Antimicrobial Resistance: What Economics Can Contribute. *Science*, **364**, eaau4679. https://doi.org/10.1126/science.aau4679

[3] Zhang, Q. and Zhang, C. (2020) Chronic Exposure to Low Concentration of Graphene Oxide Increases Bacterial Pathogenicity via the Envelope Stress Response. *Environmental Science & Technology*, **54**, 12412-12422. https://doi.org/10.1021/acs.est.0c04538

[4] Almagor, J., *et al.* (2018) The Impact of Antibiotic Use on Transmission of Resistant Bacteria in Hospitals: Insights from an Agent-Based Model. *PLoS ONE*, **13**, e0197111. https://doi.org/10.1371/journal.pone.0197111

[5] Pristov, K. and Ghannoum, M. (2019) Resistance of Candida to Azoles and Echinocandins Worldwide. *Clinical Microbiology and Infection*, **25**, 792-798. https://doi.org/10.1016/j.cmi.2019.03.028

[6] Luepke, K.H., *et al.* (2017) Past, Present, and Future of Antibacterial Economics: Increasing Bacterial Resistance, Limited Antibiotic Pipeline, and Societal Implications. *Pharmacotherapy*: *The Journal of Human Pharmacology and Drug Therapy*, **37**, 71-84. https://doi.org/10.1002/phar.1868

[7] Bonomo, R.A., *et al.* (2017) Gram-Negative Bacterial Infections: Research Priorities, Accomplishments, and Future Directions of the Antibacterial Resistance Leadership Group. *Clinical Infectious Diseases*, **64**, S30-S35. https://doi.org/10.1093/cid/ciw829

[8] Trecarichi, E., *et al.* (2016) Haematologic Malignancies Associated Bloodstream Infections Surveillance (HEMABIS) Registry—Sorveglianza Epidemiologica Infezioni Funginein Emopatie Maligne (SEIFEM) Group, Italy. Bloodstream Infections Caused by *Klebsiella pneumoniae* in Onco-Hematological Patients: Clinical Impact of Carbapenem Resistance in a Multicentre Prospective Survey. *American Journal of Hematology*, **91**, 1076-1081. https://doi.org/10.1002/ajh.24489

[9] Córdoba, G., *et al.* (2017) Prevalence of Antimicrobial Resistant *Escherichia coli* from Patients with Suspected Urinary Tract Infection in Primary Care, Denmark. *BMC Infectious Diseases*, **17**, Article No. 670. https://doi.org/10.1186/s12879-017-2785-y

[10] Zhang, X., *et al.* (2019) Colistin Resistance Prevalence in *Escherichia coli* from Domestic Animals in Intensive Breeding Farms of Jiangsu Province. *International Journal of Food Microbiology*, **291**, 87-90.

[11] Elbediwi, M., *et al.* (2019) Global Burden of Colistin-Resistant Bacteria: Mobilized Colistin Resistance Genes Study (1980-2018). *Microorganisms*, **7**, 461. https://doi.org/10.3390/microorganisms7100461

[12] Guo, Y., *et al.* (2020) Prevalence and Therapies of Antibiotic-Resistance in *Staphylococcus aureus*. *Frontiers in Cellular and Infection Microbiology*, **10**, 107. https://doi.org/10.3389/fcimb.2020.00107

[13] Kobayashi, S.D., Malachowa, N. and DeLeo, F.R. (2015) Pathogenesis of *Staphylococcus aureus* Abscesses. *The American Journal of Pathology*, **185**, 1518-1527. https://doi.org/10.1016/j.ajpath.2014.11.030

[14] Gandra, S., *et al.* (2019) The Mortality Burden of Multidrug-Resistant Pathogens in India: A Retrospective, Observational Study. *Clinical Infectious Diseases*, **69**, 563-570. https://doi.org/10.1093/cid/ciy955

[15] Shittu, A.O., *et al.* (2018) Mupirocin-Resistant *Staphylococcus aureus* in Africa: A Systematic Review and Meta-Analysis. *Antimicrobial Resistance & Infection Control*, **7**, 1-16. https://doi.org/10.1186/s13756-018-0382-5

[16] Purrello, S., *et al.* (2016) Methicillin-Resistant *Staphylococcus aureus* Infections: A Review of the Currently Available Treatment Options. *Journal of Global Antimicrobial Resistance*, **7**, 178-186. https://doi.org/10.1016/j.jgar.2016.07.010

[17] Doernberg, S.B., *et al.* (2017) Gram-Positive Bacterial Infections: Research Priorities, Accomplishments, and Future Directions of the Antibacterial Resistance Leadership Group. *Clinical Infectious Diseases*, **64**, S24-S29. https://doi.org/10.1093/cid/ciw828

[18] Cheng, M.-F., *et al.* (2005) Risk Factors for Fatal Candidemia Caused by *Candida albicans* and Non-Albicans Candida Species. *BMC Infectious Diseases*, **5**, Article No. 22. https://doi.org/10.1186/1471-2334-5-22

[19] Theuretzbacher, U., *et al.* (2020) The Global Preclinical Antibacterial Pipeline. *Nature Reviews Microbiology*, **18**, 275-285. https://doi.org/10.1038/s41579-019-0288-0

[20] Qais, F.A., *et al.* (2019) Antibacterial Effect of Silver Nanoparticles Synthesized Using *Murraya koenigii* (L.) against Multidrug-Resistant Pathogens. *Bioinorganic Chemistry and Applications*, **2019**, Article ID: 4649506. https://doi.org/10.1155/2019/4649506

[21] Monowar, T., *et al.* (2018) Silver Nanoparticles Synthesized by Using the Endophytic Bacterium *Pantoea ananatis* Are Promising Antimicrobial Agents against Multidrug Resistant Bacteria. *Molecules*, **23**, 3220. https://doi.org/10.3390/molecules23123220

[22] Numan, A.A., Ahmed, M., Mohammed, S.O., Al-Qaubti, M., Al-Tahami, K.A. and Halboup, A. (2021) Parameters' Optimization for the Green Synthesis of Silver Nanoparticles from Ziziphus spina-christi Leaves and Their Antibacterial Activities against Antibiotic Sensitive and Resistant Bacteria. *International Journal of Nanotechnology and Allied Science*, **5**, 10-25. https://journals.psmpublishers.org/index.php/ijnas/article/view/594

[23] Abdelghany, T.M., Al-Rajhi, A.M.H., Al Abboud, M.A., *et al.* (2018) Recent Advances in Green Synthesis of Silver Nanoparticles and Their Applications: About Future Directions. A Review. *BioNanoScience*, **8**, 5-16. https://doi.org/10.1007/s12668-017-0413-3

[24] Abdelghany, T.M., Abdel, R., Shater, M., Al Abboud, M.A. and Alawlaqi, M.M. (2013) Silver Nanoparticles Biosynthesis by *Fusarium moniliforme* and Their Antimicrobial Activity against Some Food-Borne Bacteria. *Mycopathologia*, **11**, 1-7.

[25] Abdelghany, T.M. (2013) *Stachybotrys chartarum*: A Novel Biological Agent for the Extracellular Synthesis of Silver Nanoparticles and Their Antimicrobial Activity. *Indonesian Journal of Biotechnology*, **18**, 75-82. https://doi.org/10.22146/ijbiotech.7871

[26] Bakri, M.M., El-Naggar, M.A., Helmy, E.A., Ashoor, M.S. and Abdel Ghany, T.M. (2020) Efficacy of *Juniperus procera* Constituents with Silver Nanoparticles against *Aspergillus fumigatus* and *Fusarium chlamydosporum*. *BioNanoScience*, **10**, 62-72. https://doi.org/10.1007/s12668-019-00716-x

[27] Ganash, M., Abdel Ghany, T.M. and Omar, A.M. (2018) Morphological and Biomolecules Dynamics of Phytopathogenic Fungi under Stress of Silver Nanoparticles. *BioNanoScience*, **8**, 566-573. https://doi.org/10.1007/s12668-018-0510-y

[28] Singh, A., *et al.* (2020) Green synthesis of Metallic Nanoparticles as Effective Alternatives to Treat Antibiotics Resistant Bacterial Infections: A Review. *Biotechnology Reports*, **25**, e00427. https://doi.org/10.1016/j.btre.2020.e00427

[29] Kim, K.-J., *et al.* (2009) Antifungal Activity and Mode of Action of Silver Nano-Particles on *Candida albicans*. *Biometals*, **22**, 235-242. https://doi.org/10.1007/s10534-008-9159-2

[30] Abdel Ghany, T.M. and Hakamy, O.M. (2014) *Juniperus procera* as Food Safe Additive, Their Antioxidant, Anticancer and Antimicrobial Activity against Some Food-Borne Bacteria. *Journal of Biological and Chemical Research*, **31**, 668-677.

[31] Harborne, A. (1998) Phytochemical Methods a Guide to Modern Techniques of Plant Analysis. Springer Science & Business Media, Berlin.

[32] Fransworth, N. (1996) Phytochemical Methods in Medicinal Research. *Journal of Pharmaceutical Sciences*, **55**, 225-269.

[33] Logeswari, P., Silambarasan, S. and Abraham, J. (2013) Ecofriendly Synthesis of Silver Nanoparticles from Commercially Available Plant Powders and Their Antibacterial Properties. *Scientia Iranica*, **20**, 1049-1054.

[34] Netai, M.-M., Stephen, N. and Musekiwa, C. (2017) Synthesis of Silver Nanoparticles Using Wild *Cucumis anguria*: Characterization and Antibacterial Activity. *African Journal of Biotechnology*, **16**, 1911-1921. https://doi.org/10.5897/AJB2017.16076

[35] Wayne, P. (2006) Performance Standards for Antimicrobial Disk Susceptibility Tests. Approved Standard, Ninth Edition. Document M2-A9. CLSI.

[36] Getasetegn, M. (2016) Chemical Composition of *Catha edulis* (khat): A Review. *Phytochemistry Reviews*, **15**, 907-920. https://doi.org/10.1007/s11101-015-9435-z

[37] Verma, A., *et al.* (2017) Optimization of Different Reaction Conditions for the Bio-Inspired Synthesis of Silver Nanoparticles Using Aqueous Extract of *Solanum nigrum* Leaves. *Journal of Nanomaterials & Molecular Nanotechnology*, **6**, 2-8. https://doi.org/10.4172/2324-8777.1000214

[38] Sanchooli, N., *et al.* (2018) *In Vitro* Antibacterial Effects of Silver Nanoparticles Synthesized Using *Verbena officinalis* Leaf Extract on *Yersinia ruckeri*, *Vibrio cholera* and *Listeria monocytogenes*. *Iranian Journal of Microbiology*, **10**, 400.

[39] Kumar, K.S. and Kathireswar, P. (2016) Biological Synthesis of Silver Nanoparticles (Ag-NPS) by *Lawsonia inermis* (Henna) Plant Aqueous Extract and Its Antimicrobial Activity against Human Pathogens. *International Journal of Current Microbiology and Applied Sciences*, **5**, 926-937. https://doi.org/10.20546/ijcmas.2016.503.107

[40] Rajan, R., *et al.* (2015) Plant Extract Synthesized Silver Nanoparticles: An Ongoing Source of Novel Biocompatible Materials. *Industrial Crops and Products*, **70**, 356-373. https://doi.org/10.1016/j.indcrop.2015.03.015

[41] Zaheer, Z. (2012) Silver Nanoparticles to Self-Assembled Films: Green Synthesis and Characterization. *Colloids and Surfaces B: Biointerfaces*, **90**, 48-52. https://doi.org/10.1016/j.colsurfb.2011.09.037

[42] Kokila, T., P. Ramesh, and D. Geetha (2015) Biosynthesis of Silver Nanoparticles from *Cavendish banana* Peel Extract and Its Antibacterial and Free Radical Scavenging Assay: A Novel Biological Approach. *Applied Nanoscience*, **5**, 911-920. https://doi.org/10.1007/s13204-015-0401-2

[43] Maria, B.S., *et al.* (2015) Synthesis of Silver Nanoparticles Using Medicinal *Zizyphus xylopyrus* Bark Extract. *Applied Nanoscience*, **5**, 755-762. https://doi.org/10.1007/s13204-014-0372-8

[44] Kajani, A.A., *et al.* (2014) Green Synthesis of Anisotropic Silver Nanoparticles with Potent Anticancer Activity Using *Taxus baccata* Extract. *RSC Advances*, **4**, 61394-61403. https://doi.org/10.1039/C4RA08758E

[45] Shehzad, A., *et al.* (2018) Synthesis, Characterization and Antibacterial Activity of Silver Nanoparticles Using *Rhazya stricta*. *PeerJ*, **6**, e6086. https://doi.org/10.7717/peerj.6086

[46] Kumar, B., *et al.* (2017) Green Synthesis of Silver Nanoparticles Using Andean Blackberry Fruit Extract. *Saudi Journal of Biological Sciences*, **24**, 45-50. https://doi.org/10.1016/j.sjbs.2015.09.006

[47] Verma, A. and M.S. Mehata (2016) Controllable Synthesis of Silver Nanoparticles Using Neem Leaves and Their Antimicrobial Activity. *Journal of Radiation Research and Applied Sciences*, **9**, 109-115. https://doi.org/10.1016/j.jrras.2015.11.001

[48] Shankar, S.S., *et al.* (2004) Rapid Synthesis of Au, Ag, and Bimetallic Au Core-Ag Shell Nanoparticles Using Neem (*Azadirachta indica*) Leaf Broth. *Journal of Colloid and Interface Science*, **275**, 496-502. https://doi.org/10.1016/j.jcis.2004.03.003

[49] Ibrahim, H.M. (2015) Green Synthesis and Characterization of Silver Nanoparticles Using Banana Peel Extract and Their Antimicrobial Activity against Representative Microorganisms. *Journal of Radiation Research and Applied Sciences*, **8**, 265-275. https://doi.org/10.1016/j.jrras.2015.01.007

[50] Vanaja, M., *et al.* (2013) Kinetic Study on Green Synthesis of Silver Nanoparticles Using *Coleus aromaticus* Leaf Extract. *Advances in Applied Science Research*, **4**, 50-55. https://doi.org/10.1007/s13204-012-0121-9

[51] Dubey, S.P., Lahtinen, M. and Sillanpää, M. (2010) Tansy Fruit Mediated Greener Synthesis of Silver and Gold Nanoparticles. *Process Biochemistry*, **45**, 1065-1071. https://doi.org/10.1016/j.procbio.2010.03.024

[52] Gan, P.P. and Li, S.F.Y. (2012) Potential of Plant as a Biological Factory to Synthesize Gold and Silver Nanoparticles and Their Applications. *Reviews in Environmental Science and Bio/Technology*, **11**, 169-206. https://doi.org/10.1007/s11157-012-9278-7

[53] Khalil, M.M., *et al.* (2014) Green Synthesis of Silver Nanoparticles Using Olive Leaf Extract and Its Antibacterial Activity. *Arabian Journal of Chemistry*, **7**, 1131-1139. https://doi.org/10.1016/j.arabjc.2013.04.007

[54] Sharma, D., Kanchi, S. and Bisetty, K. (2019) Biogenic Synthesis of Nanoparticles: A Review. *Arabian Journal of Chemistry*, **12**, 3576-3600. https://doi.org/10.1016/j.arabjc.2015.11.002

[55] Coates, J. (2006) Interpretation of Infrared Spectra, a Practical Approach. Encyclopedia of Analytical Chemistry: Applications, Theory and Instrumentation. https://doi.org/10.1002/9780470027318.a5606

[56] Smitha, S., Philip, D. and Gopchandran, K. (2009) Green Synthesis of Gold Nanoparticles Using *Cinnamomum zeylanicum* Leaf Broth. *Spectrochimica Acta Part A: Molecular and Biomolecular Spectroscopy*, **74**, 735-739. https://doi.org/10.1016/j.saa.2009.08.007

[57] Makarov, V., *et al.* (2014) "Green" Nanotechnologies: Synthesis of Metal Nanoparticles Using Plants. *Acta Naturae*, **6**, 35-44. https://doi.org/10.32607/20758251-2014-6-1-35-44

[58] Ahmad, N., *et al.* (2010) Rapid Synthesis of Silver Nanoparticles Using Dried Medicinal Plant of Basil. *Colloids and Surfaces B: Biointerfaces*, **81**, 81-86. https://doi.org/10.1016/j.colsurfb.2010.06.029

[59] Zhang, Y., *et al.* (2011) Ag@ Poly(m-phenylenediamine) Core-Shell Nanoparticles for Highly Selective, Multiplex Nucleic Acid Detection. *Langmuir*, **27**, 2170-2175. https://doi.org/10.1021/la105092f

[60] Albers, C.E., *et al.* (2013) *In Vitro* Cytotoxicity of Silver Nanoparticles on Osteoblasts and Osteoclasts at Antibacterial Concentrations. *Nanotoxicology*, **7**, 30-36. https://doi.org/10.3109/17435390.2011.626538

[61] Prakash, P., *et al.* (2013) Green Synthesis of Silver Nanoparticles from Leaf Extract of *Mimusops elengi*, Linn. for Enhanced Antibacterial Activity against Multi Drug Resistant Clinical Isolates. *Colloids and Surfaces B*: *Biointerfaces*, **108**, 255-259. https://doi.org/10.1016/j.colsurfb.2013.03.017

[62] Bin-Meferij, M.M. and Hamida, R.S. (2019) Biofabrication and Antitumor Activity of Silver Nanoparticles Utilizing Novel Nostoc sp. Bahar M. *International Journal of Nanomedicine*, **14**, 9019. https://doi.org/10.2147/IJN.S230457

[63] Mariselvam, R., *et al.* (2014) Green Synthesis of Silver Nanoparticles from the Extract of the Inflorescence of *Cocos nucifera* (Family: Arecaceae) for Enhanced Antibacterial Activity. *Spectrochimica Acta Part A*: *Molecular and Biomolecular Spectroscopy*, **129**, 537-541. https://doi.org/10.1016/j.saa.2014.03.066

[64] Jain, D., *et al.* (2009) Synthesis of Plant-Mediated Silver Nanoparticles Using Papaya Fruit Extract and Evaluation of Their Anti-Microbial Activities. *Digest Journal of Nanomaterials and Biostructures*, **4**, 557-563.

[65] Jain, S. and Mehata, M.S. (2017) Medicinal Plant Leaf Extract and Pure Flavonoid Mediated Green Synthesis of Silver Nanoparticles and Their Enhanced Antibacterial Property. *Scientific Reports*, **7**, Article No. 15867. https://doi.org/10.1038/s41598-017-15724-8

[66] Shanmuganathan, R., *et al.* (2019) Synthesis of Silver Nanoparticles and Medical Applications—A Comprehensive Review. *Current Pharmaceutical Design*, **25**, 2650-2660. https://doi.org/10.2174/1381612825666190708185506

[67] Liu, C., *et al.* (2018) Spermine Increases Bactericidal Activity of Silver-Nanoparticles against Clinical Methicillin-Resistant *Staphylococcus aureus*. *Chinese Chemical Letters*, **29**, 1824-1828. https://doi.org/10.1016/j.cclet.2018.10.025

[68] Paul, S., Mohanram, K. and Kannan, I. (2018) Antifungal Activity of Curcumin-Silver Nanoparticles against Fluconazole-Resistant Clinical Isolates of Candida Species. *Ayu*, **39**, 182. https://doi.org/10.4103/ayu.AYU_24_18

[69] Marquez, L. and Quave, C.L. (2020) Prevalence and Therapeutic Challenges of Fungal Drug Resistance: Role for Plants in Drug Discovery. *Antibiotics*, **9**, 150. https://doi.org/10.3390/antibiotics9040150

[70] Osbourn, A.E. (2003) Saponins in Cereals. *Phytochemistry*, **62**, 1-4. https://doi.org/10.1016/S0031-9422(02)00393-X